

Stability of the three-dimensional Coulomb friction law

BY HANBUM CHOT AND J. R. BARBER

Department of Mechanical Engineering and Applied Mechanics, University of Michigan, Ann Arbor, MI 48109-2125, USA

Received 19 January 1998; accepted 21 May 1998

It is known that problems arise over existence and uniqueness of solution in quasistatic contact problems involving large coefficients of Coulomb friction. This paper considers the behaviour of an elastically supported mass with three translational degrees of freedom that can make contact with a rigid Coulomb friction support. A critical coefficient of friction is identified, above which the quasi-static solution can be non-unique. A numerical solution of the corresponding dynamic problem shows that the state realized then depends on the initial conditions.

Even below the critical coefficient of friction, the dynamic solution can deviate from the quasi-static even for arbitrarily small loading rates. Typical dynamic responses include limit-cycle oscillations in velocity, oscillations involving a brief period of zero velocity (stick) and 'stick—slip' motion in which the mass spends significant periods in a state of stick, interspersed with short rapid-slip periods. All these non-steady motions involve non-rectilinear motion, even in cases where the time derivative of the applied load is constant in direction.

A perturbation analysis is performed on the quasi-static frictional slip solution and predicts instability for certain slip directions, depending on functions of the off-diagonal stiffness components and the coefficient of friction. These results are presented in dimensionless form in stability diagrams. It is also shown that quasi-static slip that is stable when there is no damping can be destabilized if the damping matrix has sufficiently large off-diagonal components.

 $Keywords:\ Coulomb\ friction;\ non-uniqueness;\ stability;\ stick-slip\ motion;\ contact$

1. Introduction

If the loading rate in an elastic contact problem is sufficiently slow, it is usually appropriate to use a quasi-static analysis in which mass is neglected and the system is assumed to pass through a sequence of equilibrium states. If Coulomb friction conditions are assumed in the contact region, i.e. if the tangential traction opposing the instantaneous motion is proportional to the local normal pressure, the quasi-static solution will depend on time, but only in a parametric sense describing the history of the loading. In other words, the same sequence of equilibrium states could be traversed at a different (not necessarily uniform) rate, without changing the quasi-static solution.

 $[\]dagger$ Present address: Mechanical Dynamics, Inc., 2301 Commonwealth Boulevard, Ann Arbor, MI 48105, USA.

Difficulties are encountered with both existence and uniqueness proofs for the general quasi-static elastic contact problem with Coulomb friction (Kikuchi & Oden 1988). Some of these difficulties can be resolved by using a non-local friction law that smoothes the discontinuities inherent in the Coulomb law. However, the uniqueness proof still requires that the coefficient of friction be sufficiently small (Oden & Pires 1983). The question of non-uniqueness of problems with Coulomb friction has been extensively studied by Klarbring (1984, 1990). In particular, he examined the behaviour of a simple two-degree-of-freedom system involving an elastically supported rigid body that can slide on a rigid plane or separate from it under the influence of applied forces. Klarbring showed that for sufficiently high coefficients of friction, loading conditions exist under which three different quasi-static states are possible: stick, slip in one direction and separation.

Cho & Barber (1998) developed a numerical simulation for Klarbring's model including dynamic effects, i.e. including the mass of the system and integrating the resulting equations of motion. They showed that in cases where the quasi-static solution is non-unique, the dynamic solution selects one of two states (stick or separation) depending on the history of the process, but the third state (slip) is never realized. They then used an analytical perturbation method to show that quasi-static slip in such conditions is always unstable in the sense that an infinitesimal perturbation from the quasi-static trajectory will grow without limit until a state change occurs either to stick or separation. Using these results, Cho & Barber (1998) were able to develop a revised quasi-static algorithm that predicts a trajectory within a bounded oscillation of the true dynamic behaviour. This revised algorithm predicts instantaneous jumps in position and state when the limiting friction condition is exceeded in one direction. A scenario involving discontinuities in displacement was also predicted by Martins and co-workers (Martins & Oden 1987; Martins et al. 1992, 1994) for the case where the mass is strictly zero, but damping is introduced into the system and then allowed to approach zero. They note that existence and uniqueness theorems can be established with arbitrary coefficient of friction if the requirement of continuity of displacement is relaxed.

In two-dimensional contact problems, the direction of frictional slip must lie in the plane, and hence, there are only two options: slip to the right or left. The contact problem is therefore piecewise linear, since all the states are governed by linear equations and nonlinearity is introduced only through the inequalities that trigger changes of state. By contrast, in three-dimensional systems, the direction of slip is a vector and the Coulomb friction requirement, that the frictional force opposes the instantaneous direction of slip, results in a fully nonlinear governing equation for slip states. This can introduce considerably more richness into the behaviour of the system. In the present paper, we shall develop a dynamic simulation for the three-dimensional equivalent of Klarbring's model and demonstrate its relationship to the simpler quasi-static formulation.

2. The three-dimensional friction model

Figure 1 shows a mass M with three translational degrees of freedom, u_1 , u_2 and u_3 , constrained to the domain $u_3 \ge 0$ by a rigid plane surface. The mass is connected to a generalized linear elastic support with stiffness and damping matrices K, B,

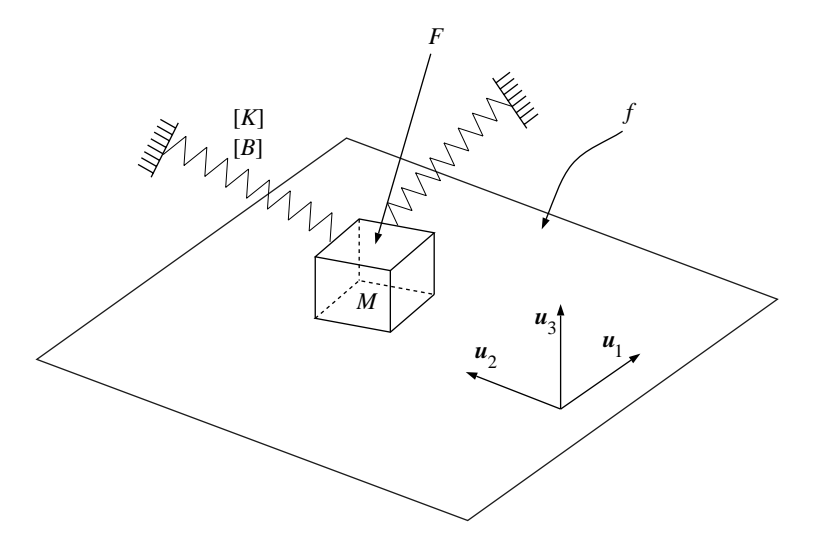


Figure 1. Three-dimensional frictional model.

respectively, and is subjected to an externally applied force F. If the mass makes contact with the plane $(u_3 = 0)$, there will also be a reaction force R.

The equation of motion of the system can be written

$$M\ddot{\boldsymbol{u}} + B\dot{\boldsymbol{u}} + K\boldsymbol{u} = \boldsymbol{F} + \boldsymbol{R}. \tag{2.1}$$

It is convenient to express some of the governing equations in component form. Latin indices will take the values 1, 2, 3 and Greek indices the values 1, 2, the summation convention being implied in each case. In this notation, equation (2.1) takes the form

$$M\ddot{u}_i + b_{ij}\dot{u}_j + k_{ij}u_j = F_i + R_i. \tag{2.2}$$

(a) States of the system

We assume unilateral contact conditions between the mass and the plane, including Coulomb friction with constant coefficient of friction f. Under these assumptions, the system can, at any given time, be in any one of the three states: separation, stick, or slip. Each of these states is governed by one or more equations and inequalities.

(i) Separation

Separation requires that the mass be above the plane, i.e.

$$u_3 \geqslant 0, \tag{2.3}$$

in which case there is no reaction between the mass and the plane, i.e.

$$R = 0. (2.4)$$

Notice that the state where $\mathbf{R} = \mathbf{0}$ and $u_3 = 0$ is included as a limiting state of separation.

(ii) Stick

Stick is defined by the condition that the mass be in contact with the plane and at rest, i.e.

$$u_3 = 0, (2.5)$$

$$\dot{\boldsymbol{u}} = \boldsymbol{0}.\tag{2.6}$$

For stick to persist, we require that the normal reaction be compressive

$$R_3 > 0, \tag{2.7}$$

and the Coulomb friction law demands that

$$\sqrt{R_1^2 + R_2^2} < fR_3. (2.8)$$

(iii) Slip

During slip, we again require

$$u_3 = 0, (2.9)$$

$$R_3 > 0,$$
 (2.10)

and the Coulomb friction law demands that the resultant frictional force be of magnitude fR_3 and in a direction opposing the instantaneous direction of motion. This in turn implies that

$$R_{\alpha} = -\frac{fR_3 \dot{u}_{\alpha}}{\sqrt{\dot{u}_1^2 + \dot{u}_2^2}}. (2.11)$$

3. The quasi-static solution

If the external force F is applied very slowly, we anticipate that the first two terms in equations (2.1) and (2.2) will be negligible, and hence, that the trajectory of the mass can be described by the simpler *quasi-static* equations

$$Ku = F + R, (3.1)$$

supplemented by the state equations (2.3)–(2.11). In this case, the mass passes through a sequence of equilibrium states and time appears only as a parameter defining the sequence of these states. We shall refer to this as the *quasi-static solution*.

The state equations can be used to determine the possible equilibrium states of the system for a given applied force \mathbf{F} . During separation, equations (2.4) and (3.1) give $\mathbf{K}\mathbf{u} = \mathbf{F}$. Solving for u_3 and using (2.3), we find that separation is possible only if

$$d_i F_i > 0, (3.2)$$

where

$$d_i = e_{ijk}k_{j1}k_{k2},\tag{3.3}$$

and e_{ijk} is the alternating tensor. The inequality (3.2) defines the region above the plane in figure 2.

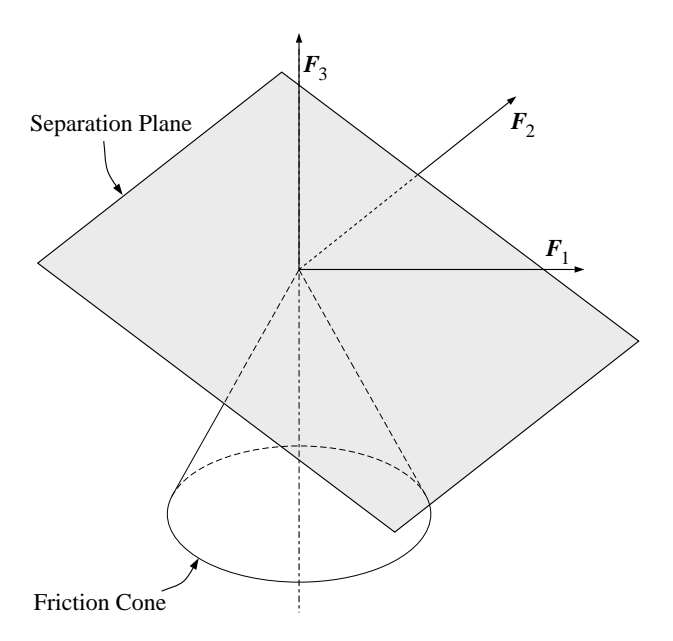


Figure 2. Three-dimensional quasi-static solution.

During stick or slip, $u_3 = 0$ and equation (3.1) can be solved for \mathbf{R} to give

$$\mathbf{R} = -\hat{\mathbf{F}},\tag{3.4}$$

where

$$\hat{F}_i = F_i - k_{i\alpha} u_{\alpha}. \tag{3.5}$$

Substitution into (2.8) then shows that stick is possible only if

$$\sqrt{\hat{F}_1^2 + \hat{F}_2^2} < -f\hat{F}_3,\tag{3.6}$$

which defines the region inside the cone in figure 2. The apex of the cone lies on the plane $d_iF_i=0$ for all u_1,u_2 .

Finally, the slip condition requires

$$\sqrt{\hat{F}_1^2 + \hat{F}_2^2} = -f\hat{F}_3,\tag{3.7}$$

corresponding to the surface of the cone in figure 2.

If the cone and the plane intersect only at the vertex as shown in figure 2, the conditions for separation and stick are mutually exclusive. However, if $f > f_{cr}$, where

$$f_{\rm cr} = \frac{d_3}{\sqrt{d_1^2 + d_2^2}},\tag{3.8}$$

an intersection can occur as shown in figure 3, giving rise to non-uniqueness of the quasi-static solution for appropriate loading histories. Similar results are obtained in two-dimensional problems for sufficiently large coefficients of friction and are discussed by Klarbring (1984) and Cho & Barber (1998).

For the present, we shall restrict attention to the case $f < f_{cr}$, for which the quasi-static solution is generally expected to be unique.

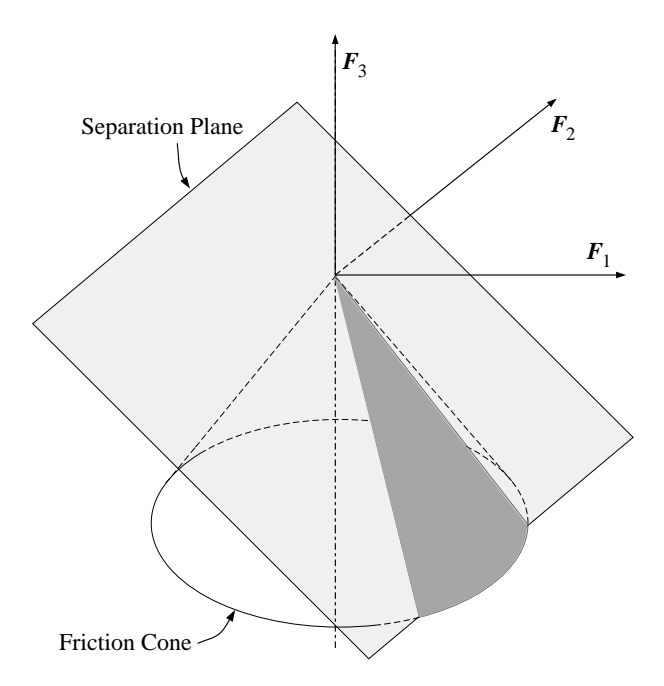


Figure 3. Three-dimensional quasi-static solution: non-unique case.

(a) Effect of loading history

Suppose the applied force F(t) is prescribed as a function of time t and we wish to determine the corresponding displacement function u(t). We anticipate that u(t) will depend on the history of loading as well as the instantaneous value F(t). In this respect, frictional contact shares some of the features of elastic-plastic problems.

Some qualitative features of the dependence on loading can be deduced directly from the above discussion. Suppose we cause a particle to move around in F-space to describe the loading history F(t). As long as the particle is inside the cone, stick occurs and the cone does not move. If we attempt to move the particle through the cone surface, slip occurs so as to keep the instantaneous point on the cone surface. The only way the particle can escape the cone is through the vertex, where a transition occurs to separation. Similarly, when the particle moves back from separation to contact, this occurs through the vertex of the cone and will involve a transition to either stick or slip depending on the direction of the local force trajectory.

(b) Rule for slip motion

When slip occurs, equation (2.11) must be used to determine the direction of the resultant motion, and hence, the motion of the friction cone in \mathbf{F} -space.

The slip equation (3.7) can be satisfied by defining

$$\hat{F}_{\alpha} = -f\hat{F}_3 n_{\alpha},\tag{3.9}$$

where n is a unit vector in the plane (i.e. $n_3 = 0$).

Suppose we now increase F by a small increment ΔF , causing a displacement increment defined by the components

$$\Delta u_{\alpha} = \Delta u \xi_{\alpha},\tag{3.10}$$

where ξ is also a unit vector in the plane. The slip rule (2.11) and equation (3.4) require that

$$\hat{F}_{\alpha} + \Delta \hat{F}_{\alpha} = -f(\hat{F}_3 + \Delta \hat{F}_3)\xi_{\alpha},\tag{3.11}$$

and we can differentiate (3.5) to obtain

$$\Delta \hat{F}_i = \Delta F_i - k_{i\alpha} \Delta u_{\alpha}. \tag{3.12}$$

Substituting for $\Delta \hat{F}_i$, Δu_{α} from (3.12) and (3.10) into (3.11), we obtain

$$\Delta F_{\alpha} + f \Delta F_{3} \xi_{\alpha} - k_{\alpha\beta} \xi_{\beta} \Delta u - f k_{3\beta} \xi_{\beta} \xi_{\alpha} \Delta u = f \hat{F}_{3} (n_{\alpha} - \xi_{\alpha}), \tag{3.13}$$

constituting two equations for the two unknowns Δu , $\boldsymbol{\xi}$. The left-hand side of this equation tends uniformly to zero as $\Delta \boldsymbol{F} \to \boldsymbol{0}$, if the quasi-static solution is continuous, and hence, in this limit we must have $\boldsymbol{n} - \boldsymbol{\xi} \to \boldsymbol{0}$. To the first order, \boldsymbol{n} and $\boldsymbol{\xi}$ are almost parallel unit vectors and we can write

$$\boldsymbol{\xi} \approx \boldsymbol{n} - \epsilon(\boldsymbol{n} \times \boldsymbol{e}_3), \tag{3.14}$$

where ϵ is a small angle that tends to zero as $\Delta F \to 0$ and e_3 is the unit vector in direction 3.

Substituting (3.14) into (3.13), and dropping second-order terms in ϵ , we obtain two equations for Δu , ϵ that can be solved for Δu to give

$$\Delta u = \frac{\Delta F_{\alpha} n_{\alpha} + f \Delta F_3}{k_{\alpha\beta} n_{\alpha} n_{\beta} + f k_{3\alpha} n_{\alpha}}.$$
(3.15)

Thus, the algorithm for slip requires that the displacement u be updated by the increment (3.15) in direction n in response to the force increment ΔF .

The numerator in (3.15) is proportional to the projection of $\Delta \mathbf{F}$ on the outward normal from the friction cone. It will therefore be positive if \mathbf{F} is changed in such a way as to try to pass outside the instantaneous surface of the cone. This is consistent with the friction law (2.11) as long as the denominator in (3.15) is positive, i.e.

$$k_{\alpha\beta}n_{\alpha}n_{\beta} + fk_{3\alpha}n_{\alpha} > 0. (3.16)$$

The stiffness matrix K is positive definite, and this guarantees that the first term in (3.16) is positive for all n, but the second term can be positive or negative and circumstances can arise in which (3.16) is violated for certain directions n. In this case, infinitesimal slip in response to an infinitesimal change in F is inconsistent with the slip rule. Since $F + \Delta F$ is outside the stick cone and below the separation plane, the conditions for stick and separation are also violated, and hence, the quasi-static solution breaks down.

It is easily shown in such cases that there exists a range of values of $\boldsymbol{u} + \Delta \boldsymbol{u}$ consistent with the new value of \boldsymbol{F} , but these positions are not in an infinitesimal neighbourhood of \boldsymbol{u} and are non-unique. Thus, we conclude that the quasi-static solution loses continuity and an indeterminate instantaneous jump in \boldsymbol{u} must occur. Generally the new state will be expected to be within the stick cone rather than on the boundary, so that motion will occur in a stick—slip mode, but the parameters of this discontinuous motion cannot be determined from the quasi-static algorithm.

It is also interesting to note that, when (3.16) is violated, a force increment to a new position *inside* the cone (for which the numerator of (3.16) is negative) will be consistent with the slip assumption, so that for such directions of loading both stick and slip can occur.

4. Dynamic solution

When the quasi-static solution predicts anomalous or paradoxical results, further insight can be obtained by returning to a full dynamic solution of the problem, using equations (2.1) and (2.2). Unfortunately, this generally necessitates a numerical solution.

(a) Numerical algorithm

The dynamic equations of motion and the state equations were integrated in time using an elementary explicit algorithm, similar to that described by Cho & Barber (1998). We suppose that the position u(t) and velocity $\dot{u}(t)$ are both known at time t and that the state of the system is also known at this time.

We assume that the state persists through the next time increment Δt , and hence, we can use the state equations (2.3)–(2.11) to determine the reaction force \mathbf{R} . The acceleration during this time increment can then be approximated as

$$M\ddot{\boldsymbol{u}} = \boldsymbol{F}(t) + \boldsymbol{R}(t) - \boldsymbol{B}\dot{\boldsymbol{u}}(t) - \boldsymbol{K}\boldsymbol{u}(t), \tag{4.1}$$

from equation (2.1).

The position and velocity at the end of the time increment is then updated as

$$\mathbf{u}(t + \Delta t) = \mathbf{u}(t) + \dot{\mathbf{u}}(t)\Delta t, \tag{4.2}$$

$$\dot{\boldsymbol{u}}(t + \Delta t) = \dot{\boldsymbol{u}}(t) + \ddot{\boldsymbol{u}}(t)\Delta t. \tag{4.3}$$

During slip periods, numerical stability is enhanced by defining the velocity vector, $\dot{\boldsymbol{u}}$, in terms of a scalar arc velocity, \dot{s} , and an instantaneous direction, $\boldsymbol{\xi}$. In this case, the update equation (4.3) takes the form

$$\dot{s}(t + \Delta t) = \dot{s}(t) + \boldsymbol{\xi} \cdot \ddot{\boldsymbol{u}}(t)\Delta t, \tag{4.4}$$

$$\boldsymbol{\xi}(t + \Delta t) = \boldsymbol{\xi}(t) + \left(\frac{\boldsymbol{\eta}(t) \cdot \ddot{\boldsymbol{u}}(t)}{\dot{\boldsymbol{s}}(t)}\right) \boldsymbol{\eta}(t) \Delta t, \tag{4.5}$$

where

$$\eta = e_3 \times \xi \tag{4.6}$$

is the in-plane unit normal to the trajectory.

Numerical experiments show that significant changes in slip direction can occur just before the mass comes to rest (and hence, changes state to 'stick'). Also, circumstances can arise in which the mass makes an almost 180° change in direction. This is the three-dimensional equivalent of the two-dimensional change from forward to backward slip. However, in three dimensions, the mass will not usually come to rest even instantaneously. Instead, the trajectory will approximate a very narrow ellipse, the arc velocity will fall to a small value near the maximum displacement point and in this region there will be rapid changes in slip direction.

In both these cases, significant errors can arise in the use of equation (4.5) because the update in ξ is insufficiently small. To avoid such errors, the dynamic algorithm adjusts the time increment in order to ensure that no more than 0.001 rad change in slip direction occurs during any one time increment.

(b) State changes

State changes are indicated when violations are detected in the inequalities (2.3), (2.8) and (2.10). When the stick inequality (2.8) is violated, slip is assumed in the direction \boldsymbol{n} as defined in equation (3.9). When the contact inequality (2.10) is violated during slip, this indicates a transition to separation.

When the separation inequality (2.3) is violated, a transition can occur to either stick or slip depending on the approach velocity $\dot{\boldsymbol{u}}(t)$. Inelastic impact conditions are assumed, so that $\dot{u}_3(t+\Delta t)$ is set to zero. This implies the occurrence of a normal impulse $-M\dot{u}_3(t)$. If a transition occurs to slip, there will also be a proportional tangential impulse and the resulting tangential velocities will be

$$\dot{u}_{\alpha}(t + \Delta t) = \dot{u}_{\alpha}(t)(1 - f\cot(\varphi)),\tag{4.7}$$

where φ is the angle of incidence defined by

$$\cos(\varphi) = -\frac{\dot{\boldsymbol{u}}(t) \cdot \boldsymbol{e}_3}{|\dot{\boldsymbol{u}}(t)|}.\tag{4.8}$$

If $f \cot(\varphi) > 1$, equation (4.7) indicates that the limiting frictional impulse is more than sufficient to bring the mass to rest, and hence, a transition to stick occurs. These rules can be given a geometrical interpretation. If the mass approaches the plane with a trajectory that, if extended below the surface, would pass inside a 'friction cone' of angle $\arctan(f)$, there will be a transition to stick. If the trajectory passes outside this cone, the transition will slip in the direction of the projection of the impact velocity on the plane, but with reduced velocity as defined by equation (4.7).

When the arc velocity \dot{s} changes sign during a time increment, this indicates a transition to stick, unless the updated position u would involve a violation of (2.8), in which case a 180° reversal of slip direction is produced by setting $\xi = -\xi$ and $\dot{s} = -\dot{s}$. However, the transition from slip to stick can also be associated with rapid changes in slip direction as explained above. During this process, the update equation (4.5) will become numerically unstable as $\dot{s} \to 0$. We therefore adopt a threshold value of \dot{s} below which the transition to stick is assumed to take place.

(c) Results

The dynamic algorithm was first used to investigate the behaviour of the system under unidirectional monotonically increasing loads. If we postulate the existence of rectilinear quasi-static slip in a given direction θ at constant normal reaction R_3 , the friction forces will not change with time and an incremental application of the equilibrium equation (3.1) will define a unique direction for the required increment of applied force. For most loading directions, the trajectory predicted by the dynamic algorithm oscillates about that predicted by the quasi-static solution, with the amplitude of the oscillation depending upon the initial conditions used. The inclusion of any amount of damping in the system causes the amplitude of this oscillation to decay with time, so that the trajectory approaches the quasi-static solution.

(i) Stick-slip motion

If the intended direction of quasi-static slip requires incremental loading that violates condition (3.16), the dynamic algorithm predicts a stick-slip motion that follows

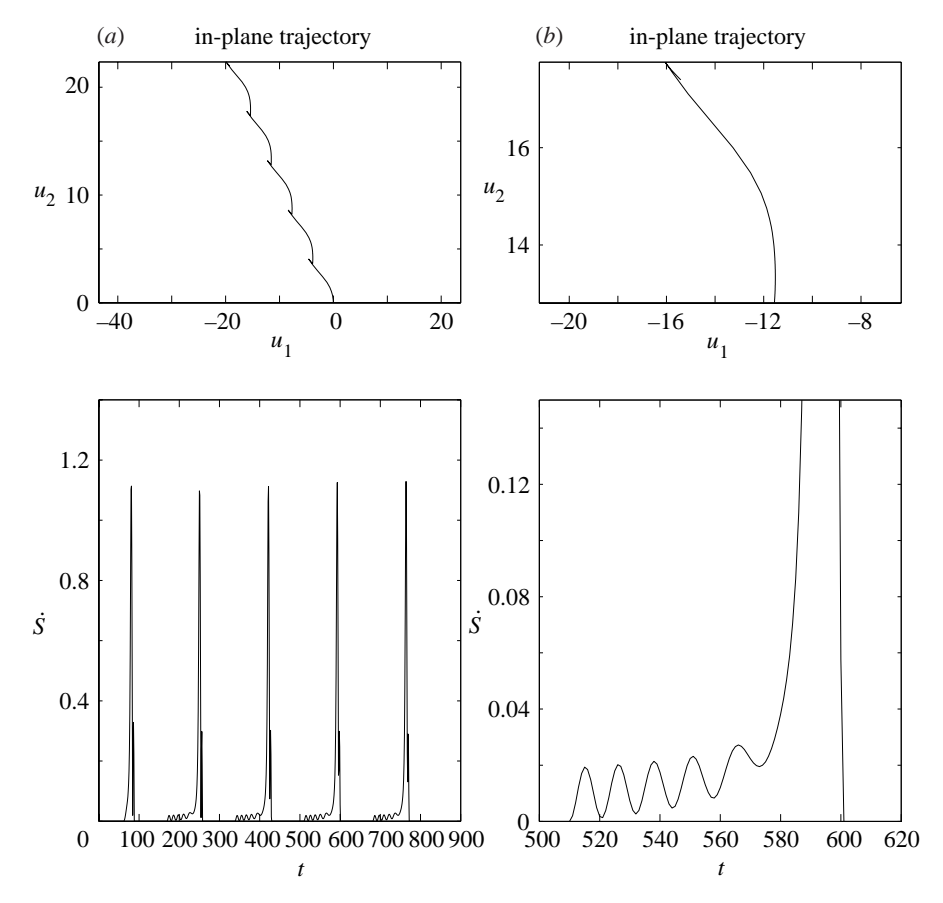


Figure 4. Stick-slip motion. (a) Trajectory and velocity. (b) Precursors.

the quasi-static trajectory only in the averaged sense that the deviation in instantaneous position is bounded in time. Figure 4a shows the variation of arc velocity with time, and the corresponding trajectory for such a case, with $\theta = \tan^{-1}(\xi_2/\xi_1) = 130^{\circ}$, f = 0.9 and

$$\mathbf{K} = \begin{bmatrix} 1 & 1 & -1 \\ 1 & 2 & -2 \\ -1 & -2 & 3 \end{bmatrix}, \quad \mathbf{B} = \mathbf{0}. \tag{4.9}$$

The mass executes a stick–slip motion, with reproducible amplitude, period and slip trajectory. Notice that the slip trajectory is a scalloped shape rather than a straight line. Indeed, we can prove that this must always be the case, since if straight line stick–slip motion were possible, it would also be describable in the two-dimensional problem of Cho & Barber (1998) and they showed that this was not a possibility. Thus, the stick–slip mechanism is intimately connected with the non-linear nature of the three-dimensional Coulomb law. Most previous explanations of experimentally observed stick–slip motion depend on the coefficient of friction being a decreasing function of sliding speed (Bell & Burdekin 1969; Armstrong-Helouvry 1991; Ibrahim 1994), but we emphasize that in the present analysis, stick–slip motion is obtained with a constant coefficient.

Figure 4b shows the arc velocity at the beginning of the slip event in more detail. Notice how the motion starts as an oscillation with the minimum speed returning almost to zero several times, until eventually a major slip event occurs. One is reminded of the precursor waves preceding earthquake events (Okamoto 1984).

The simulation results also show that stick—slip tends to occur at high normal contact force and slow sliding speed. Adams (1995) reported a similar trend in instabilities associated with the destabilization of frictional interface waves.

(ii) Oscillatory behaviour

Stick-slip motion is always obtained when the direction of slip is such that the inequality (3.16) is violated, but for some other directions of monotonic loading, steady oscillatory behaviour can be obtained. Usually, the arc velocity oscillates between a maximum value and a value very close to zero, as shown in figure 5a. Under certain circumstances there can be a period of stick at this point, but there are important differences from the stick-slip motion illustrated in figure 4. The trajectory during the oscillatory state deviates very slightly from the quasi-static, but this deviation is too small to be detectable in figure 5a. If a sufficient amount of isotropic damping $(b_{ij} = b\delta_{ij})$ is included, the oscillation is suppressed, leading to the stable response of figure 5b.

If the imposed loading is a linear function of time, the quasi-static solution involves constant velocity and hence satisfies the dynamic equations of motion, since the acceleration term is zero. Thus, by choosing appropriate initial conditions for velocity we can predispose the dynamic solution to follow the quasi-static prediction. In figure 6 we show the results of such a simulation. The system deviates rapidly from the quasi-static solution, suggesting that the latter is unstable to small perturbations. This was verified numerically at short periods of time by examining the dynamic response to small differences from the required quasi-static initial conditions. Deviation from the quasi-static solution was found to be proportional to the initial perturbation and to have the form of an exponentially growing oscillation. This suggests that additional insight into the process might be obtained by performing a perturbation analysis on the quasi-static solution. We develop such an analysis in the next section.

5. Perturbation analysis

We consider a loading scenario in which the quasi-static solution consists of steady slip with

$$u_{\alpha} = V\xi_{\alpha}t,\tag{5.1}$$

where V is a constant sliding velocity and the in-plane vector $\boldsymbol{\xi}$ defines the sliding direction. We also choose conditions such that the quasi-static normal reaction $R_3 = N$ is a constant.

The governing equations during slip can be obtained from equations (2.2) and (2.9) as

$$M\ddot{u}_{\alpha} + b_{\alpha\beta}\dot{u}_{\beta} + k_{\alpha\beta}u_{\beta} = F_{\alpha} - \frac{fR_{3}\dot{u}_{\alpha}}{\sqrt{\dot{u}_{1}^{2} + \dot{u}_{2}^{2}}},$$
(5.2)

$$b_{3\beta}\dot{u}_{\beta} + k_{3\beta}u_{\beta} = F_3 + R_3, \tag{5.3}$$

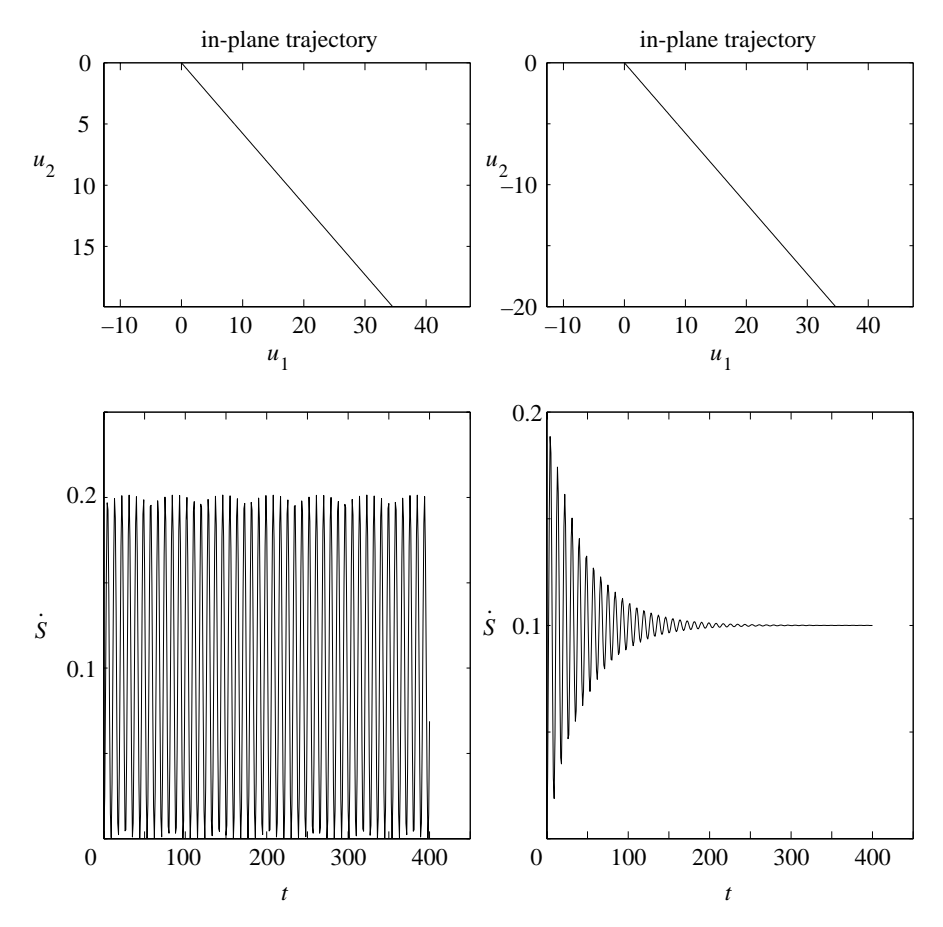


Figure 5. Oscillatory slip with zero initial velocity. (a) No damping. (b) b = 0.05.

and (5.1) will be a solution of these equations provided that

$$F_{\alpha} = b_{\alpha\beta}\xi_{\beta}V + k_{\alpha\beta}\xi_{\beta}Vt + fN\xi_{\alpha}, \tag{5.4}$$

$$F_3 = b_{3\beta}\xi_{\beta}V + k_{3\beta}\xi_{\beta}Vt - N. \tag{5.5}$$

We now define an in-plane perturbation, $V\boldsymbol{w}$, on this solution, normalized with respect to V, so that

$$u_{\alpha} = V\xi_{\alpha}t + Vw_{\alpha}. \tag{5.6}$$

Substituting this expression into (5.2)–(5.5) and eliminating F_1 , F_2 and F_3 between the resulting equations, we obtain

$$M\ddot{w}_{\alpha} + b_{\alpha\beta}\dot{w}_{\beta} + k_{\alpha\beta}w_{\beta} = \frac{fN}{V}\xi_{\alpha} - \frac{f(b_{3\beta}\dot{w}_{\beta} + k_{3\beta}w_{\beta} + N/V)(\xi_{\alpha} + \dot{w}_{\alpha})}{\sqrt{1 + 2(\xi_{1}\dot{w}_{1} + \xi_{2}\dot{w}_{2}) + \dot{w}_{1}^{2} + \dot{w}_{2}^{2}}}.$$
 (5.7)

We notice from this equation that the normalized perturbation w depends on the quasi-static sliding speed V and normal force N only through the combination N/V. It follows that the stability of quasi-static slip and the form of the nonlinear deviations from the quasi-static solution resulting in cases of instability depend on

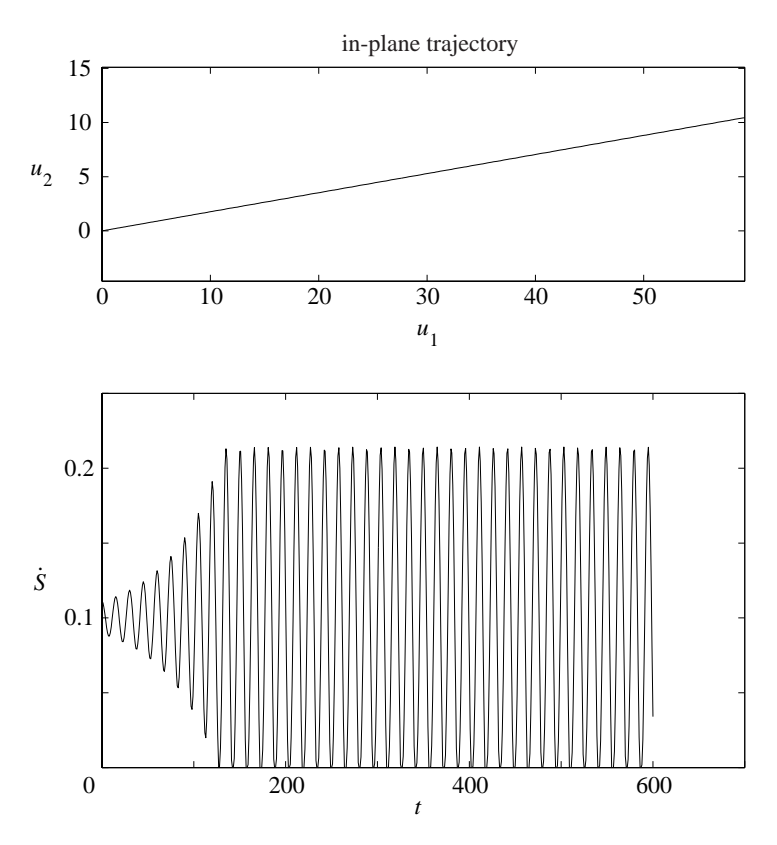


Figure 6. Oscillatory slip with quasi-static initial velocity.

speed and normal force only through this ratio. This behaviour is confirmed by numerical studies using the algorithm of $\S 4a$.

If we now restrict attention to small perturbations, so that $\dot{\boldsymbol{w}} \ll 1$, we can linearize the nonlinear term in equation (5.7) obtaining the homogeneous governing equation

$$\ddot{w}_{\alpha} + c_{\alpha\beta}\dot{w}_{\beta} + s_{\alpha\beta}w_{\beta} = 0, \tag{5.8}$$

where

$$c_{\alpha\beta} = \frac{b_{\alpha\beta}}{M} + \frac{f}{M}\xi_{\alpha}b_{3\beta} + \frac{fN}{MV}l_{\alpha\beta}, \tag{5.9}$$

$$s_{\alpha\beta} = \frac{k_{\alpha\beta}}{M} + \frac{f}{M} \xi_{\alpha} k_{3\beta}, \tag{5.10}$$

$$l_{\alpha\beta} = \eta_{\alpha}\eta_{\beta} \tag{5.11}$$

and η is defined by equation (4.6).

(a) Routh-Hurwitz criteria

To determine the stability of the system, we first cast equation (5.8) in the first-order state variable form

$$\dot{q} = Aq, \tag{5.12}$$

where $\mathbf{q} = (w_1, w_2, \dot{w}_1, \dot{w}_2)^{\mathrm{T}}$ and

$$\mathbf{A} = \begin{bmatrix} 0 & 0 & 1 & 0 \\ 0 & 0 & 0 & 1 \\ -s_{11} & -s_{12} & -c_{11} & -c_{12} \\ -s_{21} & -s_{22} & -c_{21} & -c_{22} \end{bmatrix}.$$
 (5.13)

The Hurwitz polynomial is then defined as the determinant of the matrix $(\lambda \mathbf{I} - \mathbf{A})$, i.e.

$$D(\lambda) = \lambda^4 + a_1 \lambda^3 + a_2 \lambda^2 + a_3 \lambda + a_4, \tag{5.14}$$

where

$$a_1 = c_{11} + c_{22}, (5.15)$$

$$a_2 = c_{11}c_{22} - c_{12}c_{21} + s_{11} + s_{22}, (5.16)$$

$$a_3 = c_{11}s_{22} + c_{22}s_{11} - c_{12}s_{21} - c_{21}s_{12}, (5.17)$$

$$a_4 = s_{11}s_{22} - s_{12}s_{21}. (5.18)$$

The necessary and sufficient conditions for sliding to be stable can then be written

$$a_1 > 0,$$
 (5.19)

$$a_1 a_2 - a_3 > 0, (5.20)$$

$$(a_1a_2 - a_3)a_3 - a_1^2a_4 > 0, (5.21)$$

$$a_4 > 0.$$
 (5.22)

(b) Undamped case

In the interests of simplicity, we first restrict attention to the case without damping, $b_{\alpha\beta} = 0$. Denoting the slip direction by θ , such that $\xi_1 = \cos \theta$, $\xi_2 = \sin \theta$, equations (5.9) and (5.10) take the form

$$c_{11} = \frac{fN}{MV}\sin^2\theta, \qquad c_{12} = c_{21} = -\frac{fN}{MV}\sin\theta\cos\theta, \quad c_{22} = \frac{fN}{MV}\cos^2\theta, \quad (5.23)$$

$$s_{11} = \frac{k_{11}}{M} + f \frac{k_{31}}{M} \cos \theta, \qquad s_{12} = \frac{k_{12}}{M} + f \frac{k_{32}}{M} \cos \theta,$$

$$s_{21} = \frac{k_{21}}{M} + f \frac{k_{31}}{M} \sin \theta, \qquad s_{22} = \frac{k_{22}}{M} + f \frac{k_{32}}{M} \sin \theta.$$

$$(5.24)$$

Substituting these results into (5.15)–(5.18) and then into the inequalities (5.19)–(5.22), we obtain the stability criteria

$$\frac{fN}{MV} > 0, (5.25)$$

$$\frac{fN}{M^2V}(k_{22}\cos^2\theta + k_{11}\sin^2\theta - 2k_{12}\sin\theta\cos\theta) > 0,$$
(5.26)

$$\frac{f^2 N^2}{M^4 V^2} \left[\frac{1}{2} (k_{22} - k_{11}) \sin(2\theta) + k_{12} \cos(2\theta) \right]$$

$$\times \left[\frac{1}{2}(k_{22} - k_{11})\sin(2\theta) + k_{12}\cos(2\theta) + f(k_{32}\cos\theta - k_{31}\sin\theta)\right] > 0, \quad (5.27)$$

$$\frac{1}{M^2} \left[k_{11}k_{22} - k_{12}^2 + f(k_{31}k_{22} - k_{32}k_{21})\cos\theta + f(k_{32}k_{11} - k_{31}k_{12})\sin\theta \right] > 0. \quad (5.28)$$

The unperturbed quasi-static state must have a positive normal reaction N and speed V and hence (5.25) is always satisfied. Also, (5.26) is satisfied for all θ by virtue of the requirement that the stiffness matrix be positive definite.

Condition (5.28) can be written in the form

$$d_3 > f(d_1 \cos \theta + d_2 \sin \theta), \tag{5.29}$$

using the notation (3.3). This will be satisfied for all θ if

$$d_3 > f\sqrt{d_1^2 + d_2^2},\tag{5.30}$$

and this is satisfied if $f < f_{cr}$ from (3.8), since $d_3 > 0$ for positive-definite K.

It follows that (5.27) is the only condition placing a substantive restriction on the stability of quasi-static slip for $f < f_{cr}$.

(c) Effect of slip direction

To investigate the effect of slip direction and friction coefficient on stability, we first define the stiffness parameters

$$\hat{k} = \sqrt{(\frac{1}{2}(k_{22} - k_{11}))^2 + k_{12}^2}, \qquad \tilde{k} = \frac{1}{2}(k_{11} + k_{22}), \qquad k_3 = \sqrt{k_{31}^2 + k_{32}^2}.$$
 (5.31)

Notice that k, k define the centre and the radius, respectively, of the in-plane Mohr's circle of stiffness and k_3 is the magnitude of the coupling vector $k_{3\alpha}$. All three quantities are invariant under rotation of coordinate axes in the plane and always positive.

Using this notation, condition (5.27) can be written in the form

$$\frac{f^2 N^2}{M^4 V^2} [\hat{k} \cos(2\theta - \phi_1) + f k_3 \cos(\theta - \phi_2)] \hat{k} \cos(2\theta - \phi_1) > 0,$$
 (5.32)

where

$$\tan \phi_1 = \frac{k_{22} - k_{11}}{2k_{12}}, \qquad \tan \phi_2 = -\frac{k_{31}}{k_{32}}.$$
 (5.33)

Cancelling the positive factor $f^2N^2\hat{k}^2/M^4V^2$ and defining the new angles

$$\psi = \theta - \frac{1}{2}\phi_1, \qquad \phi_3 = \frac{1}{2}\phi_1 - \phi_2,$$
 (5.34)

we can write (5.32) in the simpler form

$$\left[\cos(2\psi) + \tilde{f}\cos(\psi + \phi_3)\right]\cos(2\psi) > 0, \tag{5.35}$$

where

$$\tilde{f} = fk_3/\hat{k}. \tag{5.36}$$

It follows that the existence of unstable directions of quasi-static slip depends only on the two parameters \tilde{f} and ϕ_3 , provided that $f < f_{\rm cr}$, which in the present notation can be written

$$\tilde{f} < \tilde{f}_{cr} = \frac{\rho^2 - 1}{\sqrt{\rho^2 + 1 - 2\rho \sin(2\phi_3)}},$$
(5.37)

where

$$\rho = \tilde{k}/\hat{k}.\tag{5.38}$$

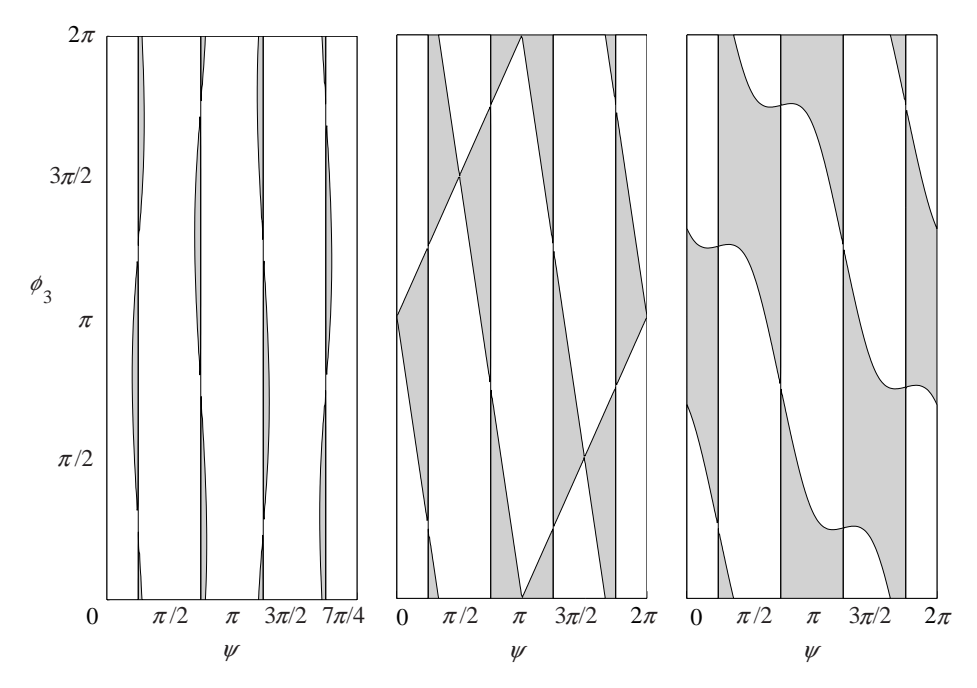


Figure 7. Stability diagram for $\tilde{f} < \tilde{f}_{\rm cr}$ (grey denotes unstable; white stable). (a) $\tilde{f} = 0.3$. (b) $\tilde{f} = 1.0$. (c) $\tilde{f} = 1.8$

Positive definiteness of the stiffness matrix K demands that $\rho > 1$.

The critical coefficient of friction depends on the angle ϕ_3 between the directions of maximum in-plane coupling and out-of-plane coupling in stiffness. However, it is clear from (5.37) that

$$\tilde{f}_{\rm cr} \leqslant \rho - 1 \equiv \tilde{f}_{\rm cr}^*,$$
 (5.39)

for all ϕ_3 and hence if the stronger condition $\tilde{f} < \tilde{f}_{\rm cr}^*$ is satisfied, (5.35) will determine the stability boundary for all ψ , ϕ_3 .

Figure 7 shows the stability chart for the undamped system derived from (5.35) for three different values of \tilde{f} . When $\tilde{f} \ll 1$, the system is stable for most directions of slip, with small regions of instability adjacent to the values $\psi = \frac{1}{4}\pi, \frac{3}{4}\pi, \frac{5}{4}\pi, \frac{7}{4}\pi$, as shown in figure 7a. These directions correspond to the principal directions of the in-plane stiffness terms. The unstable regions get larger as \tilde{f} is increased, but the character of the chart changes when $\tilde{f} = 1$, as shown in figure 7b. For $\tilde{f} > 1$, up to half of all sliding directions can be unstable depending on the value of ϕ_3 , the most unstable behaviour being obtained close to the values $\phi_3 = \frac{1}{4}\pi, \frac{3}{4}\pi, \frac{5}{4}\pi, \frac{7}{4}\pi$, as shown in figure 7c. These values correspond to the case where the out-of-plane coupling vector, $k_{3\alpha}$, is aligned with one of the principal directions of the in-plane stiffness terms. These results have been confirmed for various particular cases, using the numerical solution of § 4.

Large values of f are of course obtained when the coefficient of friction is large, but they can also be obtained for more modest coefficients if \hat{k} is small, implying that the in-plane stiffness matrix is almost isotropic. This appears to imply the paradoxical conclusion that there will be extensive instability when the in-plane stiffness matrix is

exactly isotropic. However, as \hat{k} is reduced towards zero, the exponential growth rates in unstable regions obtained from the perturbation analysis approach the imaginary axis from the right half-plane and hence predict extremely slow growth of initial perturbations. In the limit of isotropy, the corresponding quasi-static solution will be neutrally stable and any initial oscillation will tend to persist during slip.

(d) The case
$$\tilde{f} > \tilde{f}_{\rm cr}^*$$

(i) Non-uniqueness

If $\tilde{f} > \tilde{f}_{\rm cr}^*$, there will be some values of ϕ_3 (and hence some regions of the chart in figure 7) for which the quasi-static solution is non-unique. These regions are defined by the converse of (5.28), which, in the notation of equations (5.31) and (5.34), takes the form

$$\rho^2 - 1 + \tilde{f}[\rho \sin(\psi + \phi_3) - \cos(\psi - \phi_3)] > 0.$$
 (5.40)

When this condition is violated, the Routh-Hurwitz criteria show that quasi-static slip will be unstable in addition to being non-unique. In fact, numerical trials in these regions show that a transition rapidly occurs to one of the other two states—stick or separation—as in the simpler two-dimensional problem of Cho & Barber (1998).

Condition (5.40) depends on ρ as well as \tilde{f} . Figure 8 shows the stability chart obtained for $\tilde{f} = 1.8$ and various values of ρ . Non-uniqueness occurs in the approximately elliptical shaded regions centred on the points $(\psi, \phi_3) = (\frac{3}{4}\pi, \frac{3}{4}\pi), (\frac{7}{4}\pi, \frac{7}{4}\pi)$ in figure 8. These regions decrease in size as ρ increases and vanish when $\rho = \tilde{f} + 1$, which corresponds to the limiting condition $\tilde{f} = \tilde{f}_{cr}^*$, from (5.39).

(ii) Stick-slip

We also recall that continuous slip in direction ψ is possible only if condition (3.16) is satisfied, which in the present notation takes the form

$$\rho + \sin(2\psi) + \tilde{f}\sin(\psi + \phi_3) > 0.$$
 (5.41)

If this condition is not satisfied, attempts to force slip in direction ψ will result in stick–slip motion as shown in figure 4.

Notice that (5.41), like (5.40), is satisfied for all (ψ, ϕ_3) if $\tilde{f} < \tilde{f}_{\rm cr}^*$, while for $\tilde{f} > \tilde{f}_{\rm cr}^*$, there will be ranges of these parameters for which stick–slip motion occurs. These regions are bounded by the dashed curves in figure 8. Like the shaded multiple solution regions defined in § 5 d (i) above, they are centred on the points $(\psi, \phi_3) = (\frac{3}{4}\pi, \frac{3}{4}\pi), (\frac{7}{4}\pi, \frac{7}{4}\pi)$, but they are not coextensive with the multiple-solution regions. In particular, there exist ranges of parameters for which the quasi-static solution is unique for all slip directions ψ , but for which some of these directions involve stick–slip motion.

In summary, this analysis shows that both stick-slip motion and non-uniqueness can be eliminated by choosing the system parameters so that $\rho > \tilde{f} + 1$, but for all values of the parameters there will be some directions of steady quasi-static slip that are unstable and that will tend to generate oscillatory behaviour. These unstable ranges can be minimized by reducing the value of \tilde{f} , but they can only be eliminated by making the out-of-plane coupling term k_3 identically zero.

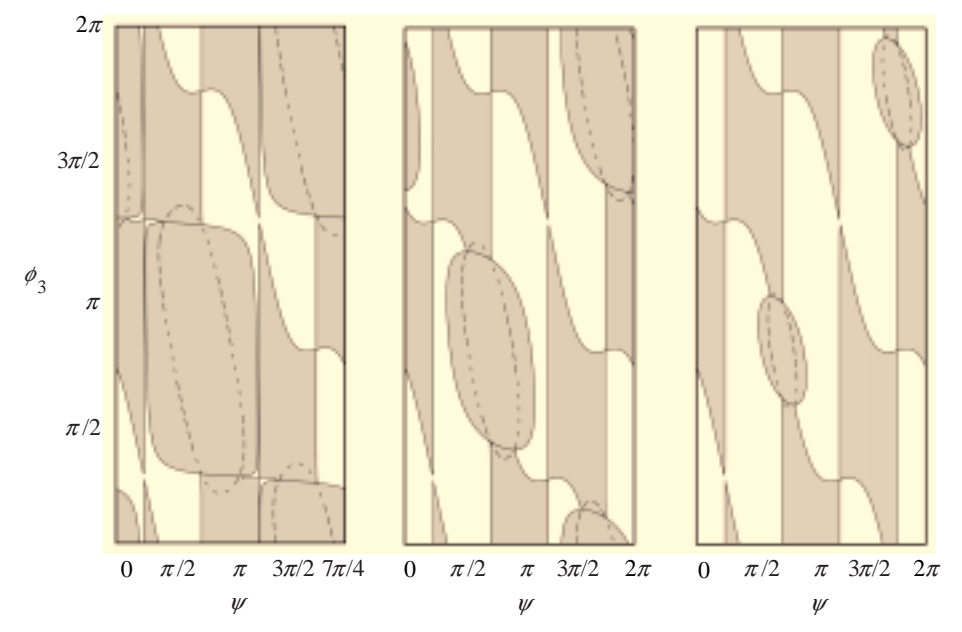


Figure 8. Stability diagram for $\tilde{f}=1.8>\tilde{f}_{\rm cr}^*$ (grey denotes unstable; white stable). (a) $\rho=1.1.$ (b) $\rho=1.8.$ (c) $\rho=2.5.$

(e) Effect of damping

All the above results relate to the undamped case. Introduction of damping to the system introduces six new parameters and greatly complicates the analysis. However, certain general features of the results can be identified.

We first note that the addition of damping terms affects only the coefficients $c_{\alpha\beta}$ in equation (5.9) and hence has no effect on the fourth Routh–Hurwitz criterion (5.18), (5.22) and (5.28), nor does it affect the stick–slip criterion (3.16). It follows that the extent of the unstable regions bounded by the quasi-elliptical and dashed curves in figure 8 are unaffected by damping, and also that damping is not an effective way of preventing stick–slip motion.

In general, we would expect the addition of damping to reduce the domain of instability defined by the remaining stability criteria and this is indeed the case for isotropic damping defined by $b_{ij} = b\delta_{ij}$, where b is a positive constant. In this case, it can once again be demonstrated that conditions (5.19) and (5.20) are unconditionally satisfied, while (5.21) can be cast in the form

$$\Omega(b^*, \tilde{N}) + \tilde{N}^2[\cos(2\psi) + \tilde{f}\cos(\psi + \phi_3)]\cos(2\psi) > 0,$$
 (5.42)

where

$$\Omega(b^*, \tilde{N}) = [4\rho + 2\tilde{f}\sin(\psi + \phi_3)](b^*)^4 + [8\rho + 2\sin 2\psi + 5\tilde{f}\sin(\psi + \phi_3)]\tilde{N}(b^*)^3
+ [5\rho + 3\sin 2\psi + 4\tilde{f}\sin(\psi + \phi_3)]\tilde{N}^2(b^*)^2
+ [\rho + \sin 2\psi\tilde{f}\sin(\psi + \phi_3)]\tilde{N}^3b^*
+ [\tilde{f}^2\sin^2(\psi + \phi_3) + 4\tilde{f}\cos(\psi - \phi_3) + 4](\tilde{N}b^* + (b^*)^2),$$
(5.43)

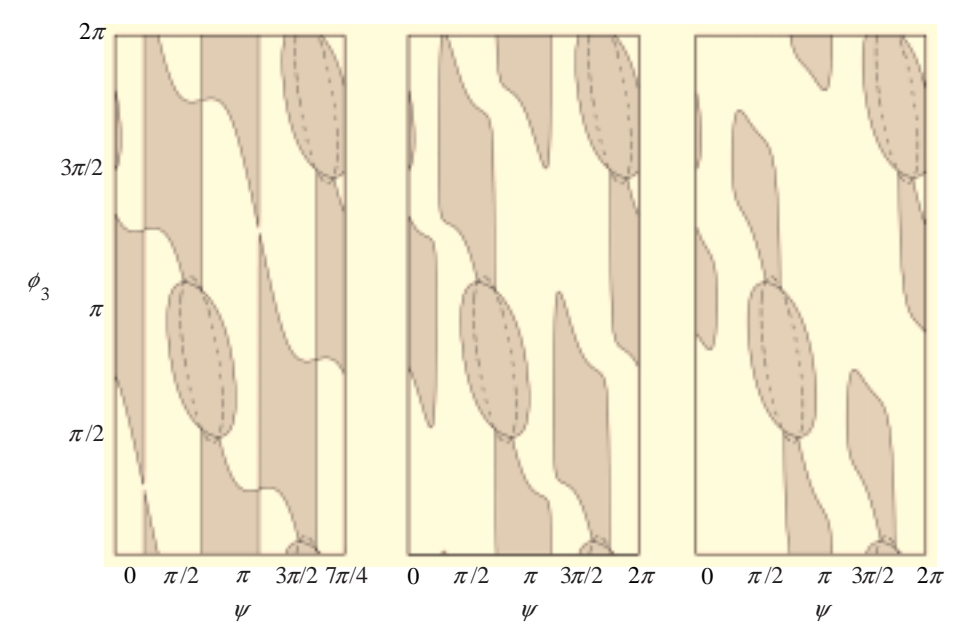


Figure 9. Stability diagram with isotropic damping ($\tilde{f} = 1.8$, $\rho = 2.2$, $\tilde{N} = 4.0$). (a) $b^* = 0.0$. (b) $b^* = 0.01$. (c) $b^* = 0.05$.

and

$$b^* = \frac{b}{\sqrt{\hat{k}M}}, \qquad \tilde{N} = \frac{fN}{V\sqrt{\hat{k}M}}.$$
 (5.44)

It can be shown that Ω is a monotonically increasing function of b^* for physically meaningful values of the other parameters and it follows that the addition of isotropic damping always shrinks the domain of instability associated with this criterion.

This effect is illustrated in figure 9, which shows the unstable domains for $\tilde{f} = 1.8$, $\rho = 2.2$, $\tilde{N} = 4.0$ and various values of b^* . Notice how the multiple solution and stick—slip domains remain unchanged, but the remaining unstable domains, governed by criterion (5.21) shrink with increasing isotropic damping.

The function $\tilde{N}^{-2}\Omega(b^*,\tilde{N})$ is unbounded at $\tilde{N}\to 0$ and $\tilde{N}\to \infty$ and exhibits a minimum between these extremes for non-zero b^* . For a given value of isotropic damping, it follows that the domains of instability due to criterion (5.21) first grow and then shrink with increasing normal load.

If the damping is not isotropic, it is easily demonstrated by counter-example that damping does not necessarily exert a stabilizing influence on the system. For example, the first Routh-Hurwitz criterion (5.19) then takes the form

$$2\tilde{b}^* + fb_3^* \cos(\theta - \phi_4) + \tilde{N} > 0, \tag{5.45}$$

where

$$\tilde{b}^* = \frac{1}{2}(b_{11}^* + b_{22}^*), \qquad b_3^* = \sqrt{b_{31}^{*2} + b_{32}^{*2}}, \qquad \tan \phi_4 = -\frac{b_{31}^*}{b_{32}^*},$$
 (5.46)

and there will be some sliding directions θ for which this criterion is violated if

$$fb_3^* > 2\tilde{b}^* + \tilde{N}.$$
 (5.47)

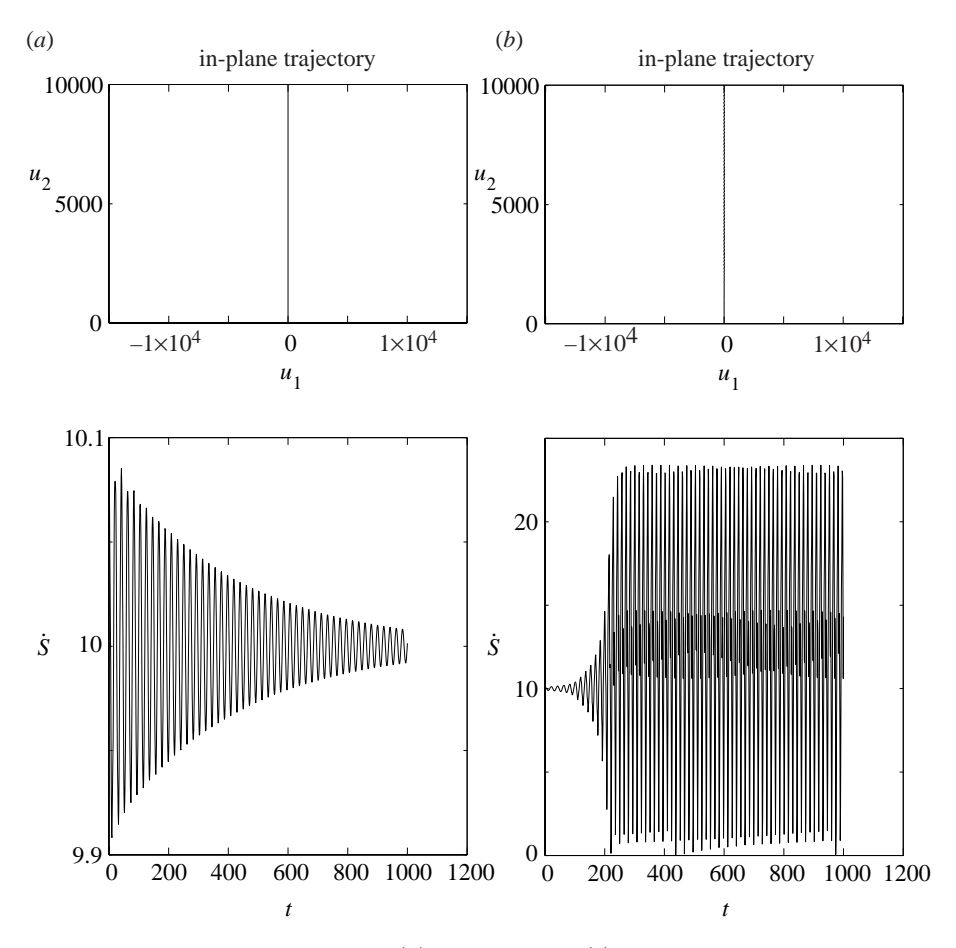


Figure 10. Destabilization by damping. (a) No damping. (b) $b_{11} = b_{22} = 0.01$, $b_{12} = 0$, $b_{31} = 0$, $b_{32} = -0.05$, $b_{33} = 0.3$.

Similar considerations apply to criteria (5.20) and (5.21) and all are associated with critical levels of the coupling term b_3^* .

This conclusion is confirmed by the simulation results. For example, figure 10 shows the transient response of the system with (a) zero damping and (b) $b_{11} = b_{22} = 0.01$, $b_{12} = 0$, $b_{31} = 0$, $b_{32} = -0.05$, $b_{33} = 0.3$ for the case where $\theta = 90$, N = 0.5, V = 10.0, f = 0.9, $u_1(0) = 0.0$, $u_2(0) = 10.1$. $\tilde{N} = 0.0426$, $\rho = 1.3416$, $\tilde{f} = 1.8$, $\psi = 0.8154$, $\phi_3 = 3.8371$.

6. More general loading trajectories

The quasi-static solution is a rigorous analytical solution of the full dynamic equations if and only if the load increases linearly with time and hence \dot{F} is a constant. For all other cases, the quasi-static solution is generally expected to approximate the dynamic behaviour if the loading rate is sufficiently small and there are no rapid changes of direction in $\dot{F}(t)$.

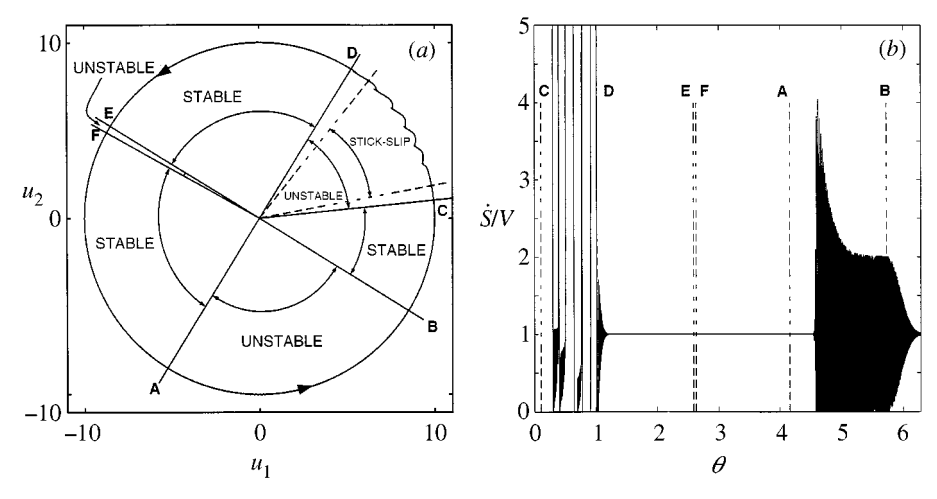


Figure 11. Stability on circular path.

Similar considerations apply to the stability analysis of § 5. Thus, for a loading scenario in which \dot{F} varies slowly, we anticipate that unstable perturbations on the quasi-static response will grow whenever the instantaneous loading direction is predicted to be unstable by conditions (5.19)–(5.22). However, the extent of such disturbances may be limited if the period of time spent in the unstable range is restricted.

Figure 11 shows a typical case in which forces are applied so as to cause the mass to execute a uniform circular motion $(u_1 = 10\cos\theta, u_2 = 10\sin\theta, \theta = 0.001t, N = 0.2, f = 0.9)$ at a slow constant speed V = 0.01. The mass follows the quasistatic trajectory closely except in the sectors AB, CD, EF, where conditions (5.19)–(5.22) indicate instability. In the sector CD, stick–slip motion is generated and there is visible deviation from the intended circular trajectory, as shown in figure 11a. In AB and EF, oscillatory motion develops as in the example of figure 6. In these sectors, the deviation from the circular trajectory is too small to be seen in figure 11a, but the instantaneous arc velocity \dot{s} deviates significantly from the intended uniform quasi-static value V, as shown in figure 11b.

Figure 12 shows a scenario in which the mass is required to execute a sudden change of direction through a small radius of curvature a. The system parameters are similar to those used for the previous example and the forces are chosen to define a quasi-static motion at constant speed V, starting with an extended straight-line segment at $\theta = 90^{\circ}$ and ending with a straight-line segment at $\theta = 180^{\circ}$. Both these line segments correspond to stable directions for this system, but the transition radius carries the mass briefly through directions for which quasi-static slip is unstable.

Figure 12 shows the resulting trajectory and arc velocity for three different values of the quasi-static velocity V. For high velocities (e.g. V=1.0, figure 12a), there is significant deviation from the intended trajectory, including a brief period of separation ($u_3 > 0$). However, these excursions are associated with dynamic (inertia) effects and decrease as the speed is reduced to V=0.1 as shown in figure 12b, though the variation in arc velocity is still significant in this case. Further reduction in velocity to V=0.01 (figure 12c) causes the deviations to increase once again, this time due to instability of the quasi-static solution while the system executes the transition radius. The slower the speed V, the longer the system resides in the range of unsta-

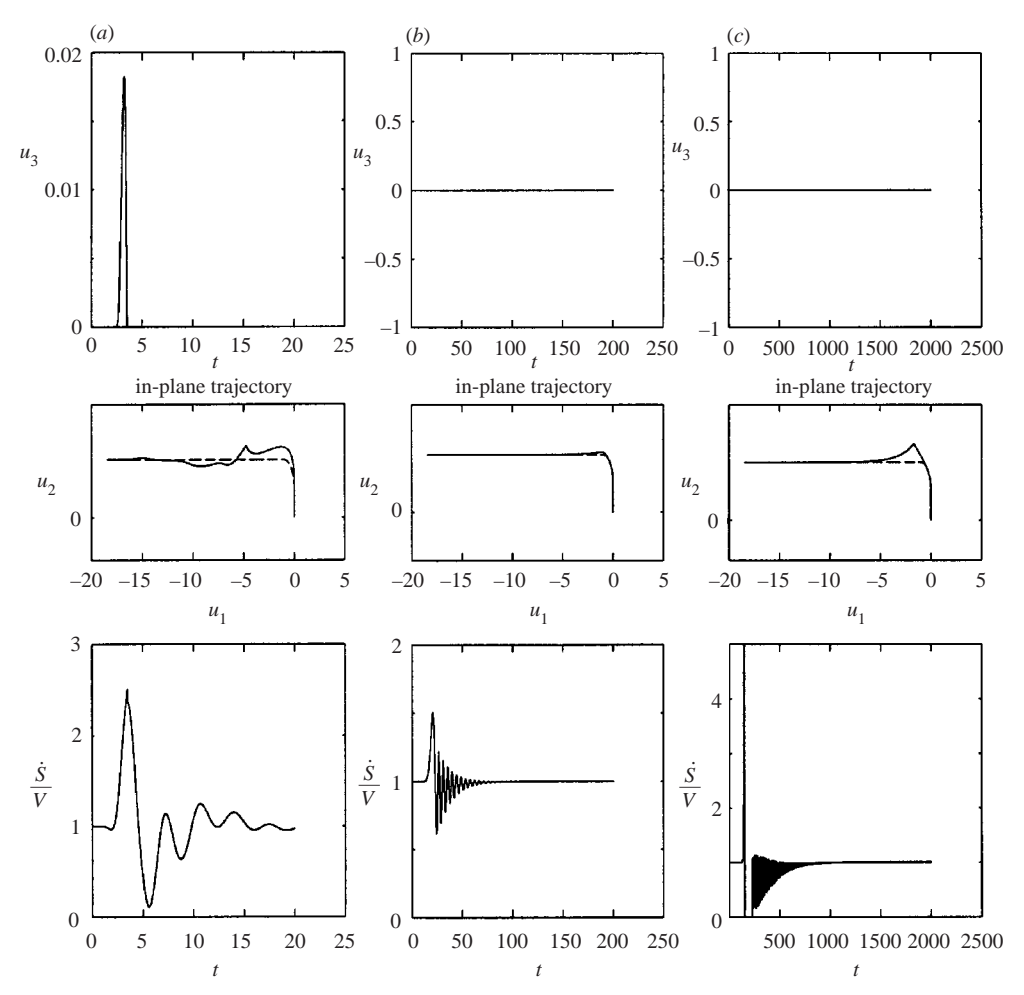


Figure 12. Quick turning through unstable region ($N=1.0,\ f=0.9,\ a=1.0$). (a) V=1.0. (b) V=0.1. (c) V=0.01.

ble slip directions, thus permitting stick—slip or oscillatory behaviour to develop. We conclude that undesirable excursions are liable to occur at both high and low quasi-static velocities, the optimum condition being obtained at intermediate values of V.

These results are clearly of concern for the control of positioning mechanisms involving Coulomb friction supports, particularly in view of the observation from figure 7 that some sliding directions are unstable even at relatively low values of \tilde{f} .

7. Conclusions

This investigation has shown that elastic systems involving three-dimensional Coulomb friction support can exhibit considerably more complex behaviour than corresponding two-dimensional systems. A critical coefficient of friction can be identified, above which the quasi-static solution is non-unique, but even below this value, some sliding directions are generally unstable, providing only that there is some cou-

pling between displacements in the sliding plane and spring forces normal to that plane. The parameter \tilde{f} determining the extent of these unstable ranges can be substantial even for low coefficients of friction if the in-plane stiffness matrix is close to isotropic. Off-diagonal terms in the damping matrix can also destabilize the system in some cases.

A numerical solution for the dynamic behaviour of the system shows that various kinds of unstable response are possible, including limit-cycle oscillations in velocity, oscillations involving a brief period of zero velocity (stick) and 'stick—slip' motion in which the mass spends significant periods in a state of stick, interspersed with short rapid slip periods. All these non-steady motions involve non-rectilinear motion, even in cases where the time derivative of the applied load is constant in direction. It should be emphasized that stick—slip motion in this system can be produced with a constant coefficient of friction, in contrast to most previous models of this phenomenon that involve a coefficient that varies with speed or a distinction between static and dynamic coefficient.

These results are of concern for the control of positioning mechanisms involving Coulomb friction support.

The authors are pleased to acknowledge support from the Automotive Research Center at the University of Michigan, a US Army Centre of Excellence in Modeling and Simulation of Ground Vehicles, under contract no. DAAE07-94-C-R094.

References

- Adams, G. G. 1995 Self-excited oscillations of two elastic half-spaces sliding with a constant coefficient of friction. ASME J. Appl. Mech. 62, 867–872.
- Armstrong-Helouvry, B. 1991 Control of machines with friction. Dordrecht, The Netherlands: Kluwer.
- Bell, R. & Burdekin, M. 1969 A study of the stick-slip motion of machine tool feed drives. Proc. Inst. Mech. Engng 184, 543-560.
- Cho, H. & Barber, J. R. 1998 Dynamic behavior and stability of simple frictional systems. Math. Comput. Modelling 28, 37–53.
- Ibrahim, R. A. 1994 Friction-induced vibration, chatter, squeal, and chaos. II. Dynamics and modeling. ASME Appl. Mech. Rev. 47, 227–253.
- Kikuchi, N. & Oden, J. T. 1988 Contact problems in elasticity: a study of variational inequalities and finite element methods. Philadelphia, PA: SIAM.
- Klarbring, A. 1984 Contact problems with friction. PhD thesis, Linköping University, Sweden. Klarbring, A. 1990 Examples of non-uniqueness and non-existence of solutions to quasi-static
- contact problems with friction. *Ingenieur-Archiv.* **60**, 529–541.

 Martins, J. A. C. & Oden, J. T. 1987 Existence and uniqueness results for dynamic contact problems with non-linear normal and friction interface laws. *Nonlinear Analyis* **11**, 407–428.
- Martins, J. A. C., Montiero Marques, M. D. P., Gastaldi, F. & Simões, F. M. F 1992 A two degree-of-freedom 'quasistatic' frictional contact problem with instantaneous jumps. In *Contact Mechanics Int. Symp., Lausanne, Switzerland,* pp. 217–228. Presses polytechniques et universitaires romande.
- Martins, J. A. C., Montiero Marques, M. D. P. & Gastaldi, F. 1994 On an example of non-existence of solution to a quasistatic frictional contact problem. *Eur. J. Mech.* A 13, 113–133.
- Oden, J. T. & Pires, E. 1983 Nonlocal and nonlinear friction laws and variational principles for contact problems in elasticity. *ASME J. Appl. Mech.* **50**, 67–76.
- Okamoto, S. 1984 Introduction to earthquake engineering, 2nd edn. University of Tokyo Press.

		·	
1		I	
•		1	